Pertanika J. Sci. & Technol. 30 (3): 1771 - 1787 (2022)

PERTANIKA JOURNALS

SCIENCE & TECHNOLOGY

Journal homepage: http://www.pertanika.upm.edu.my/

Mathematical Models for Predicting the Mechanical Properties of Poly(Lactic Acid) for Load-Bearing Applications

Abraham Aworinde[1]*, Titus Ajewole[2], Olakunle Olukayode[3] and Joseph Dirisu[1]

[1]*Department of Mechanical Engineering, College of Engineering, Covenant University, Ota 112233, Nigeria*
[2]*Department of Electrical and Electronic Engineering, Osun State University, Osogbo 230262, Nigeria*
[3]*Department of Mechanical Engineering, Osun State University, Osogbo 230262, Nigeria*

ABSTRACT

In order to widen the areas of application of poly (lactic acid) (PLA), there has been a multiplicity of experiments. This study attempts to develop mathematical models for predicting the mechanical properties of PLA to reduce the number of experimental runs and material wastage. The melt-cast method produced unreinforced PLA samples with different slenderness ratios (λ) in triplicate using. The samples were subjected to a compression test to obtain the mechanical properties captured at three main points on the stress-strain curve: yield, ultimate stress, and fracture. Regression models were developed from the data obtained at the three points, and their validity was examined by testing them against the previous relevant experimental studies from various authors. The coefficient of determination (R^2) and coefficient of correlation (ρ) was also examined for each model to establish their degree of correctness further. Analyses show that the developed models give reasonable approximations of some of the properties examined. The mass (M) and the modulus of elasticity (E) were the most accurately predictable properties with [R^2, ρ] of [99.97%, 0.9998] and [91.55%, 0.9568], respectively. Results also show that apart from the melt-cast method, the compressive modulus of PLA (both circular and rectangular cross-sections test samples) produced via injection molding and fused filament fabrication can be predicted with near accuracy using the model developed in this study. This study gives researchers the tools needed to avoid material wastage by having close-to-real values of the mechanical properties of PLA through prediction before carrying out any experiment.

Keywords: Compressive modulus, fused deposition modeling, processing technologies, regression models, sample size effect, slenderness ratio

ARTICLE INFO

Article history:
Received: 18 October 2021
Accepted: 16 December 2021
Published: 20 April 2022

DOI: https://doi.org/10.47836/pjst.30.3.02

E-mail addresses:
abraham.aworinde@covenantuniversity.edu.ng (Abraham Aworinde)
titus.ajewole@uniosun.edu.ng (Titus Ajewole)
olakunle.kayode@uniosun.edu.ng (Olakunle Olukayode)
joseph.dirisu@covenantuniversity.edu.ng (Joseph Dirisu)
* Corresponding author

ISSN: 0128-7680
e-ISSN: 2231-8526

INTRODUCTION

Polylactide has become a widely applied biopolymer. Several studies have reported its application in cardiovascular devices (Hadasha & Bezuidenhout, 2018), skeletal tissues (Aworinde et al., 2020a; Ferrer et al., 2018), drug delivery (Li et al., 2018; Tyler et al., 2016), commodities and specialties (Malinconico et al., 2018), sensing (Tajitsu, 2017), and automotive (Bouzouita et al., 2017). Its application is gaining an incredible increase in biomedical recently (Aworinde et al., 2020a; Aworinde et al., 2021a; Deepthi et al., 2016; Wang et al., 2016). Its future applications abound because of its propensity to replace many materials in the near future (Anderson & Shenkar, 2021; Cooper, 2013). It is consistent that, unlike synthetic polymers, biopolymers are generally environmentally benign (Abioye & Obuekwe, 2020; Adegbola et al., 2020; Mansour et al., 2020) and possess structural applications. For instance, a recent consideration has been given to PLA as a replacement for metals as internal bone fixation to avoid problems such as hardware pain, elastic modulus mismatch, temperature sensitivity, and others. Another emerging application of PLA is in the renewable energy field. Wind energy is one of the green energy sources already on a commercial scale and is expected to expand in the future. When the turbine structures reach their end of service life, their fabrication materials must be recyclable to be totally green. The turbine blades are made up of thermosetting fiber-reinforced polymers, which are very difficult to recycle because of the materials' nature and complex composition (Rahimizadeh et al., 2019). A study considered thermal and mechanical recycling methods in reclaiming glass fibers from end-of-life wind turbine blades (Rahimizadeh et al., 2020). It was reported that short glass fibers from blades of decommissioned wind turbines were recovered and mixed with a polylactic acid (PLA) matrix through a double extrusion process to prepare novel composite filaments for Fused Deposition Modeling (FDM).

Successful applications of PLA in various fields require that test samples of different configurations be obtained and tested in the laboratory before it is made available for end-users. In other to obtain these various test samples, a number of processing techniques are employed. These techniques include electrospinning, melt electro-writing, melt casting, and solvent casting (Aworinde et al., 2018; Gbenebor et al., 2018a; Jamshidian et al., 2010). The tests samples produced by the techniques mentioned above have been subjected to tests such as hydrophobicity (Aworinde et al., 2020b; Sundar et al., 2021), morphology (Taleb et al., 2021), rheology (Fang & Hanna, 1999; Rokbani & Ajji, 2018), and thermal (Taleb et al., 2021). Of all the tests carried out on PLA, its mechanical properties appear to be its most evaluated property (Adeosun et al., 2016; Akpan et al., 2019; Aworinde et al., 2019; Aworinde et al., 2020c; Aworinde et al., 2020a; Aworinde et al., 2021b; Brischetto & Torre, 2020; Deepthi et al., 2016; Wang et al., 2016). The mechanical test becomes necessary whenever PLA is applied as a load-bearing structure by the rule of thumb. The load-bearing samples vary in thickness, length, and shape, as shown in Table 1 and Figures 1-3, depending on the applications.

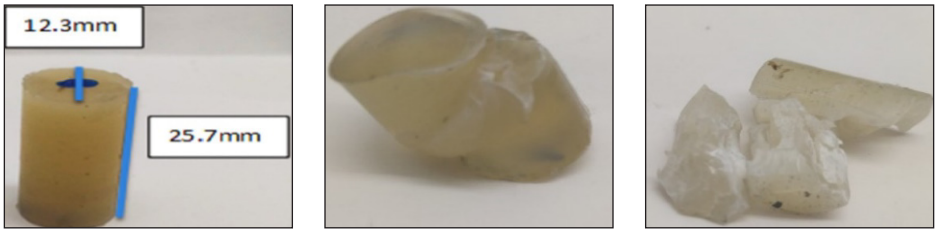

(a) (b) (c)

Figure 1. Compression sample of unreinforced PLA: (a) before testing (b) buckled after testing (c) fractured after testing (Barkhad et al., 2020)

Figure 2. Tensile test samples of PLA composites (Farah et al., 2016)

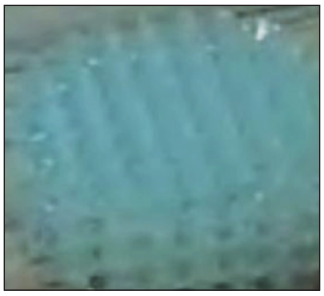

Figure 3. Compression samples from a laser-cut, 3D printed PLA (Rodrigues et al., 2016)

Table 1
Variations in the sizes of the mechanical test sample

Reference	Method of sample production	Sample's cross-section	Type of mechanical sample	Type of mechanical test	λ
(Aworinde et al., 2020a)	Melt casting	circle	Cylinder	Compression	2.24
(Akpan et al., 2019)	Electrospinning	Rectangle	Fiber mat	Tensile	n/a
(Brischetto & Torre, 2020)	Fused deposition modeling	Rectangle	Rectangular prism	Compression	10.90
(Abbas et al., 2017)	Fused deposition modeling	Rectangle	Rectangular prism	Compression	6.92
(Barkhad et al., 2020)	Injection molding	circle	Cylinder	Compression	8.36
(Gbenebor et al., 2018b)	Electrospinning	Rectangle	Fiber mat	Tensile	n/a
(Oksiuta et al., 2000)	Extrusion	n/a	Dog bone	Tensile	n/a
(Farah et al., 2016)	Hot press	n/a	Dog bone	Tensile	n/a

The compression test is one of the most frequently performed mechanical tests for obtaining the mechanical properties of PLA. Generally, the compression test has several advantages over other mechanical tests. Aside from the fact that various properties can be obtained from its result, compression test samples are very easy to fabricate. In addition, there is no limit to the extent to which the stress/strain relationship can be obtained since

the test sample is usually loaded between two relatively rigid flat platens (Figure 4), which removes the possibility of any constraints in movement until the specimen fractures (Williams & Gamonpilas, 2008). Studies show that the simplicity and versatility of the compression test have attracted researchers to its usage in determining the mechanical properties of PLA and PLA composites (Abbas et al., 2017; Aworinde et al., 2020a; Barkhad et al., 2020). This study, therefore, attempted a means of minimizing material and time wastage by providing regression models that predict some of the properties of PLA, which are obtainable via compression test.

MATERIALS AND METHOD

Polylactide (PLA) with an overall lactide purity ≥ 99.5% and monomer's molecular weight of 144 g/mol was purchased from NatureWorks, USA. It was pre-dried in an oven at 50 ^{o}C for 6 hours to eliminate the possible moisture content to forestall viscosity degradation and possibly significantly impact the mechanical properties (Lawrence et al., 2001). The moisture-free PLA was then processed using melt casting and mold pressing at the pouring temperature of 210 ^{o}C. Solid cylinders with a constant diameter of 13.28 mm and arithmetic progressively varying heights according to Equation 1 were developed. In Equation 1, l_n is the length of an nth term of a sample while a is the starting length, i.e., 9.4 mm. c is the positive constant difference between any two successive lengths, and n denotes the nth term. Three samples were produced for each length. Care was taken to keep all lengths within the prescription of ASTM D695 to avoid buckling during the mechanical test. However, there was chipping off of some samples during testing (Figure 4), which possibly impacted the linearisation of the mechanical properties.

$$l_n = \alpha + c(n-1) \tag{1}$$

The masses of the samples (triplicate) of each length were measured. The samples were afterward subjected to a compression test using a double column Instron universal testing machine with model number 3369 (equipped with Bluehill software for data acquisition) located at the Centre for Energy Research and Development (CERD) at Obafemi Awolowo University, Ile-Ife in Nigeria. The samples were axially loaded as stipulated by ASTM D695 and used in many studies (Abbas et al., 2017; Aworinde et al., 2020a; Bakar et al., 2003). The mean values of the masses, and all the compressive mechanical properties examined via experiment, were reported. The moduli of elasticity were obtained using MATLAB R2019a (9.6) to find the slope within the elastic region. Table 2, in addition to the mass, lists the compressive mechanical properties obtained from the test. These properties were considered at three main regions on the stress-strain curve (i.e., yield, ultimate or maximum stress, and break) to account for the responses of the samples when loaded in compression.

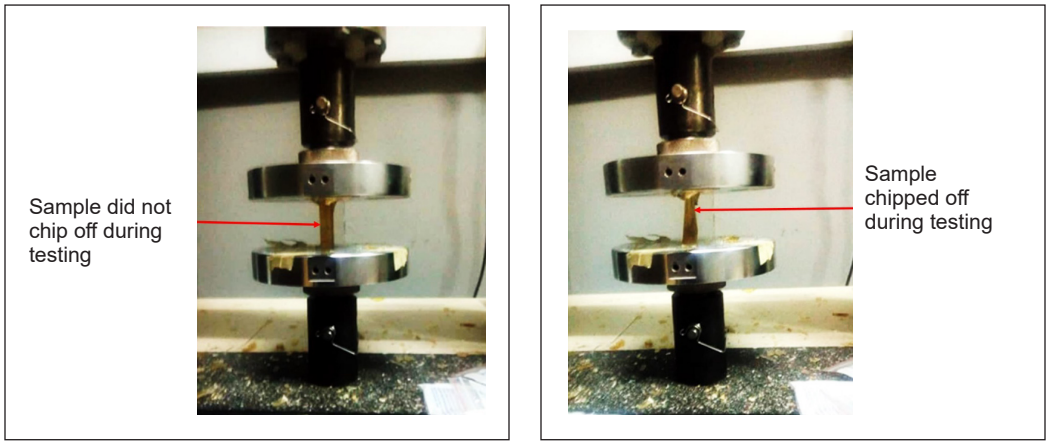

Figure 4. Chipping off of samples during compression test: (a) no chipping (b) sample chipped off

Mathematical functions were generated for each property to examine their dependence on the slenderness ratio, λ. The coefficient of determination, R^2, was also generated for each property to establish the proportion of the variance in these properties that can be predicted from the independent variable, λ.

RESULTS AND DISCUSSION

Table 2 displays the mechanical and the physical (i.e., mass) properties. The values of R^2 are also shown in Table 2. The R^2 values show that the dependence of all the examined properties on the independent variable, λ, was supported by at least 70% of the experimental data. Mass, modulus of elasticity, compressive extension at the break, ductility, compressive extension at maximum compressive stress, and compressive strain at maximum compressive stress were related to the λ and had 99.97%, 91.55%, 93.66%, 97.38%, 93.14% and 94.38 % degree of predictability, respectively, using the experimental values obtained in this study. Compressive stress and load at break were 84.79% predictable. Compressive stress and load at maximum compressive stress were 79.29% predictable, compressive stress and load at yield were 71.29% predictable. In comparison, energies at maximum compressive stress and break had 77.98% and 74.23% predictive extent of accuracy, respectively.

Figure 5 shows changes in length and mass as a function of the slenderness ratio. The length is not the focus here; hence it was not modeled since it was a predetermined factor (Equation 1) and not one of the study's outputs. Mass (M), on the other hand, was modeled by Equation 2. The model showed a fairly linear relationship. The R^2 value of 99.97% and coefficient of correlation of 0.9998 imply a reasonable degree of accuracy of values that can be predicted by Equation 2. The implication of Equation 2 is that the approximate amount of mass of PLA can be reasonably predicted, given λ. It would, in turn, help to know the

Table 2
Mechanical and physical properties of Polylactide obtained from the compression test and direct measurement

Mechanical and physical properties	Unit	Symbol	R^2	correlation (ρ)
Maximum compressive stress	MPa	σ_{UCS}	0.7929	0.7075
Compressive strain at maximum compressive stress	%	ε_{UCS}	0.9438	-0.7419
Energy at maximum compressive stress	J	U_{UCS}	0.7798	0.7472
Compressive load at maximum compressive stress	N	F_{UCS}	0.7929	0.7075
Compressive extension at maximum compressive stress	mm	e_{UCS}	0.9314	0.6182
Compressive stress at break	MPa	σ_b	0.8479	0.7933
Compressive load at break	N	F_b	0.8479	0.7933
Compressive strain at break, i.e., ductility	%	ε_b	0.9738	-0.8024
Compressive extension at break	mm	e_b	0.9366	0.6067
Energy at break	J	U_b	0.7423	0.7308
Compressive stress at yield	MPa	σ_y	0.7129	0.4492
Compressive load at yield	N	F_y	0.7129	0.4492
Modulus	MPa	E	0.9155	0.9568
Mass	g	M	0.9997	0.9998

financial implication of the mass needed for a known λ to be produced for a compression test. Although melt blending and injection molding processes have been copiously used to fabricate PLA and its composites (Aworinde et al., 2020a; Mofokeng et al., 2012), these processes have not been developed like fused deposition modeling (FDM) in terms of parametric modeling.

$$M = 0.5653\lambda + 0.0228 \quad (2)$$

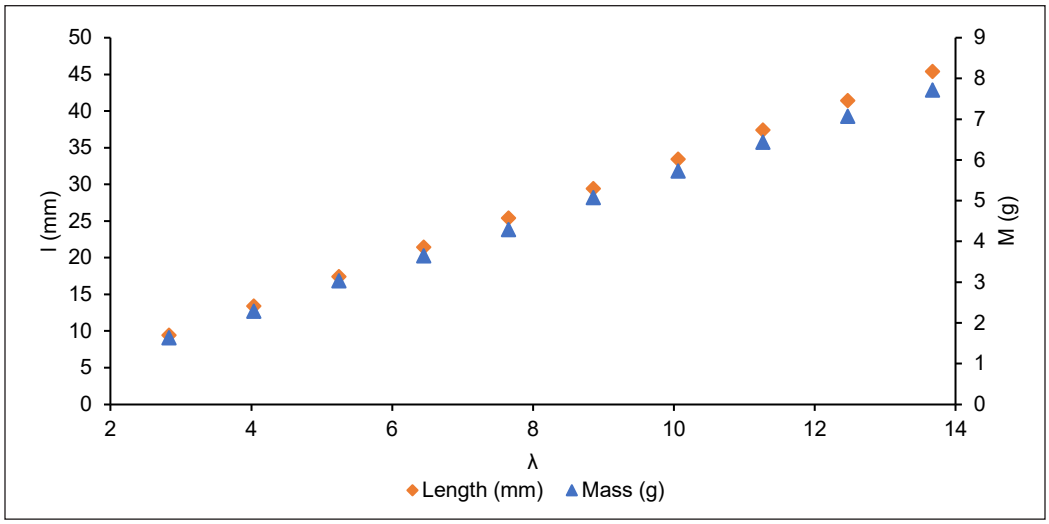

Figure 5. Samples' mass and length as affected by the slenderness ratio

Mechanical Properties at Yield

Figures 6 and 7 capture the mechanical properties of the samples at yield. Figure 6 summarizes the stress-strain responses of the samples to the compressive load within the elastic region. Equations 3 to 5 are the polynomial functions intended for predicting the elastic modulus (E), compressive load (F_y), and compressive stress (σ_y), respectively. These properties are the responses of the axially loaded PLA samples within the region where the deformation was only elastic. For example, with Equation 3, the modulus of elasticity could be predicted with 91.95% accuracy using a polynomial regression model of order one.

$$E = 226.63\lambda + 43.19 \tag{3}$$

$$F_y = 0.9395\lambda^6 - 47.833\lambda^5 + 965.26\lambda^4 - 9812.2\lambda^3 + 52559\lambda^2 - 139070\lambda + 142304 \tag{4}$$

$$\sigma_y = 0.0068\lambda^6 - 0.3453\lambda^5 + 6.9688\lambda^4 - 70.841\lambda^3 + 379.45\lambda^2 - 1004\lambda + 1027.4 \tag{5}$$

The examination of Equation 3 shows some degree of reliance in the light of other studies. Our previous work, for instance, with λ equal to 2.2 for an unreinforced sample of PLA, conforms with the model in Equation 3 (Aworinde et al., 2020a). Equation 3 also reasonably approximates the compressive modulus of elasticity of 3D printed PLA (with λ = 12.6) reported by other researchers (Brischetto & Torre, 2020). Another study equally corroborates the validity of Equation 3 (Barkhad et al., 2020). The study reports E = 1.75 GPa for unreinforced PLA (with λ = 8.36), while Equation 3 gives E = 1.94 GPa for the same value of λ. The validity of Equation 3, as further proven by its coefficient of correlation (ρ) of 0.9568, established a stately model for predicting the modulus of elasticity without any experimental setup and material wastage, given a known value of λ. Interestingly, λ can be easily determined without any recourse to experimental trials. Table 3 summarises the correlation between experimental reports and predicted values by the regression model of Equation 3. The small differences between the experimental and the predicted values could be due to the formation of pores/voids in the fabrication method (i.e., melt casting), especially as the sample's size increased.

Figure 7 shows the compressive load (F_y) and strength (σ_y) at yield. The load at yield heralds the onset of plastic deformation. After the load at yield, the load value ceases to travel in a straight line. Both properties (i.e., load and strength at yield) have the same curve pattern. Equations 4 models the relationships between λ and F_y, while Equation 5 models the relationships between λ and σ_y. The sixth (6^{th}) order that approximates these relationships shows that the polynomial regression models may not be very reliable and that the relationships may not truly exist. The correlation coefficient (Table 2) that linearly

relates F_y and σ_y to λ was 0.4492, indicating a weak correlation. It implies then that, unlike what was obtainable in the prediction of M and E, the linear relationships that connect F_y and σ_y to λ may not be properly predicted by the regression models of Equations 4 and 5. However, Figure 7 shows that the same variational pattern exists between λ and F_y and between λ and σ_y.

Table 3
Extent of the accuracy of Equation 3 in the light of experimental reports

Reference	Method of sample production	Sample's cross-section	Type of mechanical test	λ	Modulus from experiment	Modulus from Equation 3
(Aworinde et al., 2020a)	Melt casting	cylinder	Compression	2.24	522.18 MPa	550.84 MPa
(Barkhad et al., 2020)	Injection molding	cylinder	Compression	8.36	≈1750.00 MPa	1937.82 MPa
(Brischetto & Torre, 2020)	FDM	rectangle	Compression	10.90	2093.00 MPa (100%*)	2513.46 MPa

* = Infill Density

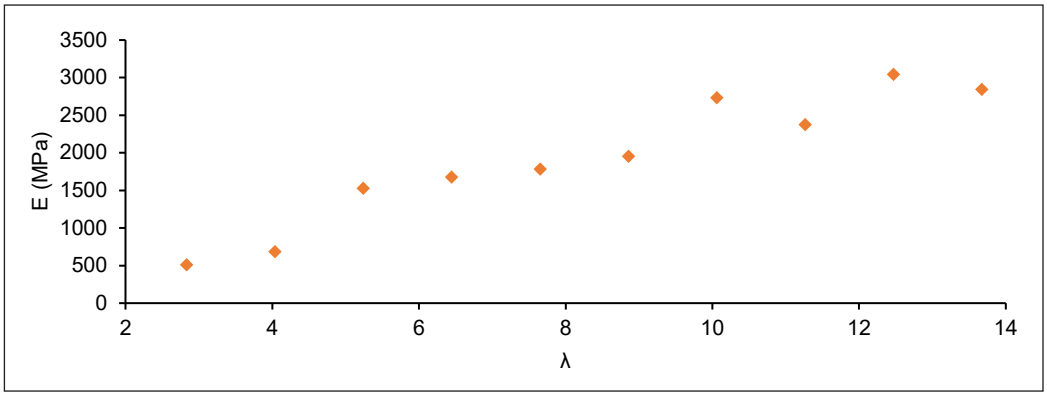

Figure 6. Dependence of modulus of elasticity on slenderness ratio

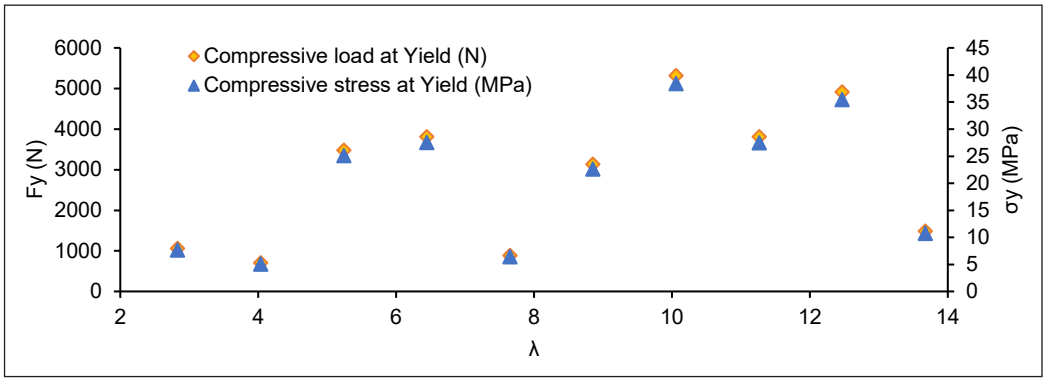

Figure 7. Predictive model of compressive load and stress at yield by slenderness ratio

Mechanical Properties at Ultimate Compressive Strength (UCS)

Figures 8-10 show the variations of the mechanical properties of PLA relative to the λ at maximum compressive strength, i.e., ultimate compressive stress (UCS). Figure 8 and Equations 6 and 7 detail the effect of λ on the compressive load (F_{UCS}) and compressive stress (σ_{UCS}) of PLA at UCS. F_{UCS}, which is the load that produces σ_{UCS}, is usually not the subject of many experimental reports. σ_{UCS}, however, has been reported for various materials (Akpan et al., 2019; Aworinde et al., 2020a; Brischetto & Torre, 2020; Gbenebor et al., 2018b), being the maximum stress any material can withstand before breaking. The values of R^2 (79.29%) and the coefficient of correlation (0.7075) show that the obtained regression model (Equation 7) is a little reliable. In the light of experimental reports, Table 2 shows the extent of accuracy of the regression model for the prediction of σ_{UCS} and the values obtained from various research reports.

$$F_{UCS} = 0.8301\lambda^6 - 42.692\lambda^5 + 873.54\lambda^4 - 9030.3\lambda^3 + 49256\lambda^2 - 132529\lambda + 137624 \quad (6)$$

$$\sigma_{UCS} = 0.006\lambda^6 - 0.3082\lambda^5 + 6.3066\lambda^4 - 65.195\lambda^3 + 355.61\lambda^2 - 956.81\lambda + 993.59 \quad (7)$$

The strain (ε_{UCS}) and the extension (e_{UCS}) at the maximum compressive stress in Figure 9 and the energy (U_{UCS}) at maximum compressive stress in Figure 10 are usually not the subjects of intense discussion when it comes to the mechanical properties of PLA. Figure 10 depicts the energy absorbed by the samples when the stress is maximum. It also describes the work done by the uniaxial compressive load as the compressive stress reaches the maximum value. As shown in Table 2, the correlation coefficient between λ and ε_{UCS} is negative. It implies a decrease in λ as ε_{UCS} increases and vice versa. The extent of reliability of Equations 8, 9, and 10 are 94.38%, 93.14%, and 77.98%, respectively (Table 2). The regression models at maximum compressive stress were evaluated at degree 6 polynomial functions. This degree substantially impacted their degree of accuracy (Sun et al., 2014; Ye & Zhou, 2013), as seen in Table 4.

$$\varepsilon_{UCS} = 0.0006\lambda^6 - 0.0336\lambda^5 + 0.719\lambda^4 - 7.846\lambda^3 + 45.541\lambda^2 - 131.8\lambda + 152.75 \quad (8)$$

$$e_{UCS} = 0.0001\lambda^6 - 0.0069\lambda^5 + 0.1471\lambda^4 - 1.5823\lambda^3 + 9.0269\lambda^2 - 25.409\lambda + 27.903 \quad (9)$$

$$U_{UCS} = 0.0003\lambda^6 - 0.0144\lambda^5 + 0.3047\lambda^4 - 3.2328\lambda^3 + 18.024\lambda^2 - 49.392\lambda + 51.873 \quad (10)$$

Table 4
Extent of the accuracy of Equation 7 in the light of experimental reports

Reference	Method of sample production	Type of mechanical test	Sample's cross-section	λ	Ultimate strength from the experiment	Ultimate strength from Equation 7
(Abbas et al., 2017)	3D printing	Compression test	rectangle	6.92	27.5 Mpa (65*)	27.38 MPa
(Aworinde et al., 2020a)	Melt casting	Compression test	circle	2.24	24.75 MPa	44.04 MPa
(Barkhad et al., 2020)	Injection molding	Compression test	circle	8.36	≈58 MPa	24.06 MPa

* = Infill Density

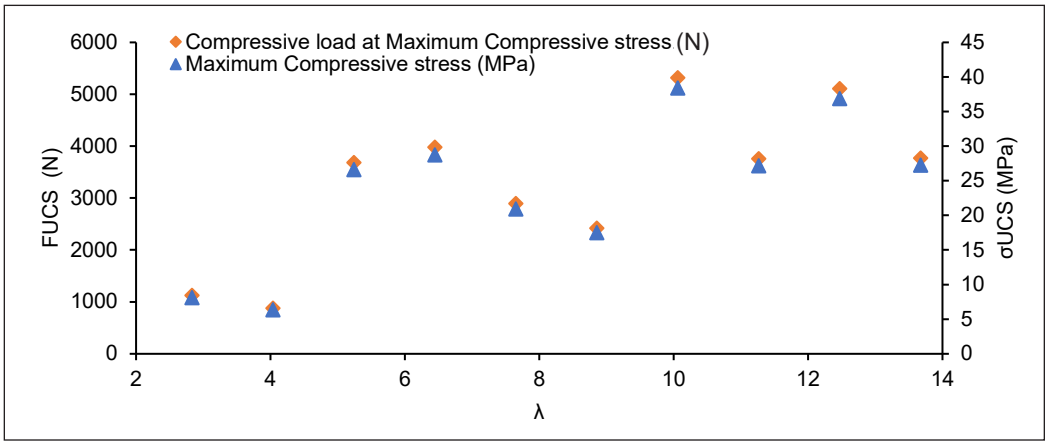

Figure 8. Dependence of compressive load and stress at UCS on slenderness ratio

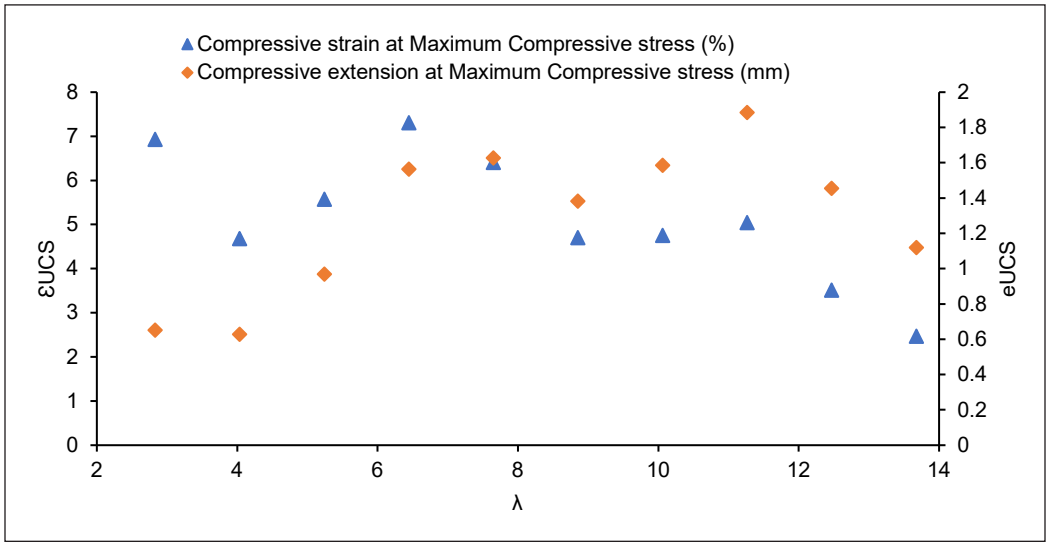

Figure 9. Pattern of compressive strain and extension at UCS as affected by slenderness ratio

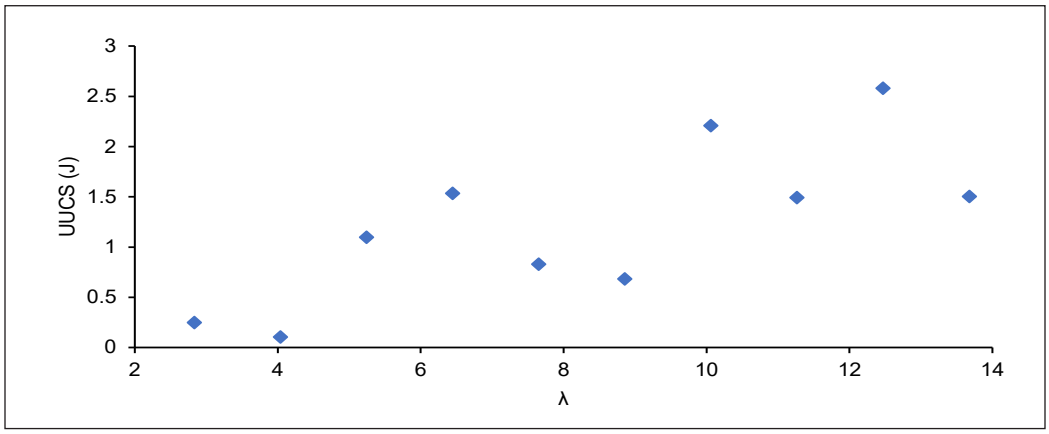

Figure 10. Energy at UCS as affected by the slenderness ratio

Mechanical Properties at Break

Five properties were evaluated at the break. Figure 11 shows the compressive load (F_b) and compressive stress (σ_b) with their regression models in Equations 11 and 12, respectively. In Figure 12, compressive strain (ε_b) and extension (e_b) are displayed, while Equations 13 and 14 model their data. Finally, the variation of energy at the break with λ is shown in Figure 13 with its corresponding regression model in Equation 15.

$$e_b = 0.0002\lambda^6 - 0.0085\lambda^5 + 0.1775\lambda^4 - 1.8896\lambda^3 + 10.696\lambda^2 - 30.002\lambda + 32.954 \quad (11)$$

$$F_b = 0.4872\lambda^6 - 25.653\lambda^5 + 536.83\lambda^4 - 5666.2\lambda^3 + 31469\lambda^2 - 85779\lambda + 89864 \quad (12)$$

$$\sigma_b = 0.0035\lambda^6 - 0.1852\lambda^5 + 3.8757\lambda^4 - 40.908\lambda^3 + 227.19\lambda^2 - 619.29\lambda + 648.78 \quad (13)$$

$$\varepsilon_b = 0.0008\lambda^6 - 0.0428\lambda^5 + 0.9093\lambda^4 - 9.8517\lambda^3 + 56.934\lambda^2 - 164.85\lambda + 191.35 \quad (14)$$

$$\mathrm{U}_b = 0.0004\lambda^6 - 0.0198\lambda^5 + 0.4098\lambda^4 - 4.2711\lambda^3 + 23.469\lambda^2 - 63.636\lambda + 66.415 \quad (15)$$

The most relevant mechanical properties at fracture are usually ε_b, also known as ductility, and U_b. Also known as fracture energy, U_b has been researched to expand the application of PLA (Noori, 2019) as it directly reflects the crack resistance of any material (Xu et al., 2018). Also, several reports have been on the ductility of PLA, which detail the outcome of various fabrication methods and the attendant effects on ductility (Adeosun et al., 2016; Akpan et al., 2019; Aworinde et al., 2019). In consonance with various studies, PLA was brittle (Nagarajan et al., 2016; Song et al., 2014). A study reported the ductility of melt-cast PLA with λ=2.24 to be 13.71% (Aworinde et al., 2019), while Equation 14

gives the ductility of the same sample size as 17.61%. Table 2 shows that Equation 14 is 97.38% reliable with a coefficient of correlation of 0.8024, which implies a strong inverse relationship between sample size and ductility. As a result of this inverse relation, increased ductility leads to decreased strength (Lascano et al., 2019).

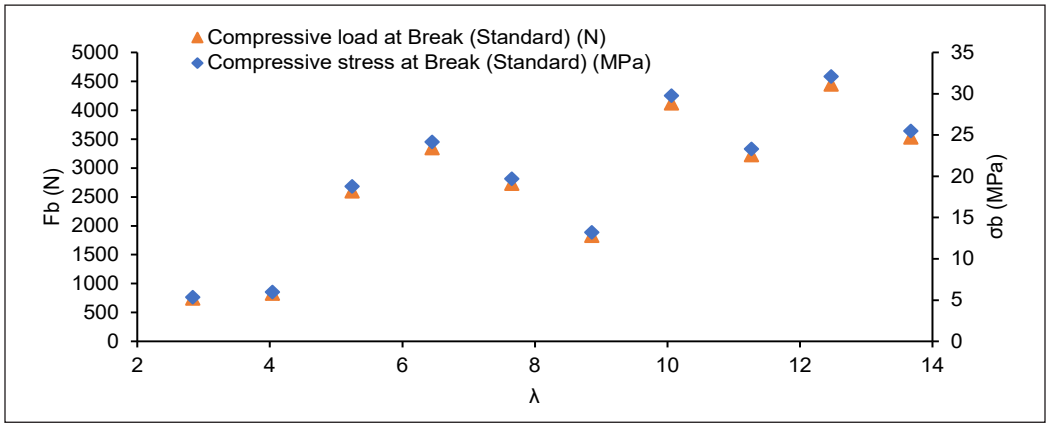

Figure 11. Compressive load and stress dependence on slenderness ratio

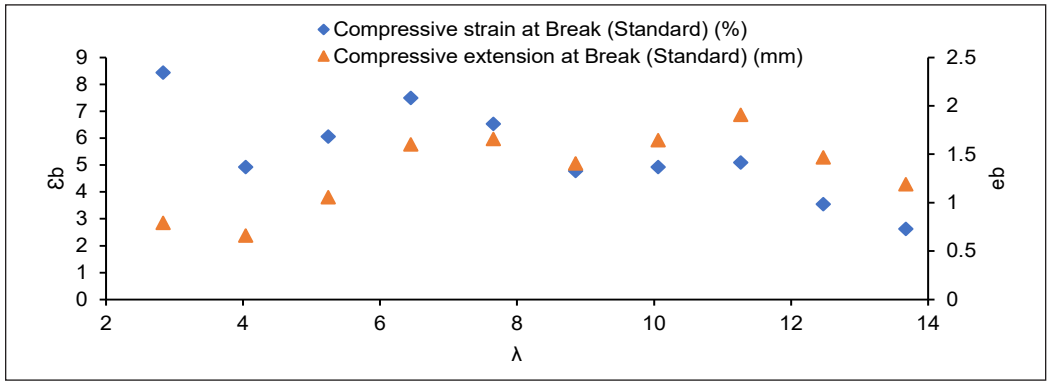

Figure 12. Compressive strain and extension at fracture as affected by slenderness ratio

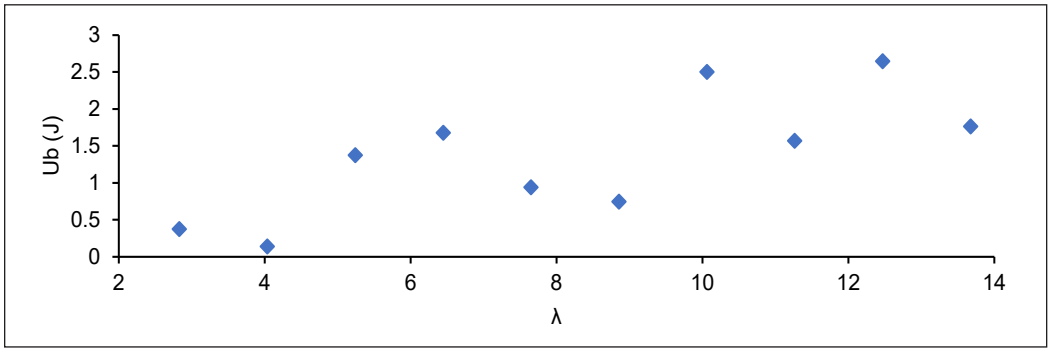

Figure 13. Energy at the break due to the growth in sample size

CONCLUSION

Regression models for predicting the mechanical properties of uniaxially compressed poly(lactic acid) samples have been developed in this study. The study was targeted toward fine-tuning experiments to manage time and resources effectively. Out of all the models developed, regression models for predicting the mass and the modulus of elasticity are the most accurate. The modulus of elasticity's regression model agrees well with the experimental results from the various relevant studies. The study revealed a strong correlational and causal relationship between the slenderness ratio of PLA and the mass of the sample. If the mass of PLA needed for an experiment can be reasonably predicted, the cost of the material can be estimated without any trial-and-error or experimental setup. Also, the study showed that the compressive modulus of elasticity of PLA could be predicted with about 92% accuracy with a known value of the slenderness ratio. In addition, the model for predicting the elastic modulus of PLA samples fabricated via melt casting (as shown in this study) can also predict the compressive modulus of PLA samples obtained via fused deposition modeling (FDM) and injection molding processes. Besides, the models developed in this work can be used to build software that predicts the mechanical properties of PLA obtainable from compression tests, which will help minimize the number of experimental runs, thereby cutting down on time, money, and material wastage.

ACKNOWLEDGEMENT

The authors wish to thank Covenant University for supporting the publication.

REFERENCES

Abbas, T., Othman, F. M., & Ali, H. B. (2017). Effect of infill parameter on compression property in FDM Process. *International Journal of Engineering Research and Application*, *7*(10), 16-19. https://doi.org/10.9790/9622-0710021619

Abioye, A. A., & Obuekwe, C. C. (2020). Investigation of the biodegradation of low-density polyethylene-starch Bi-polymer blends. *Results in Engineering*, *5*, Article 100090. https://doi.org/10.1016/j.rineng.2019.100090

Adegbola, T. A., Agboola, O., & Fayomi, O. S. I. (2020). Review of polyacrylonitrile blends and application in manufacturing technology: Recycling and environmental impact. *Results in Engineering*, *7*, Article 100144. https://doi.org/10.1016/j.rineng.2020.100144

Adeosun, S. O., Aworinde, A. K., Diwe, I. V., & Olaleye, S. A. (2016). Mechanical and microstructural characteristics of rice husk reinforced polylactide nanocomposite. *The West Indian Journal of Engineering*, *39*(2), 63-71.

Akpan, E. I., Gbenebor, O. P., Igogori, E. A., Aworinde, A. K., Adeosun, S. O., & Olaleye, S. A. (2019). Electrospun porous bio-fibre mat based on polylactide/natural fibre particles. *Arab Journal of Basic and Applied Sciences*, *26*(1), 225-235. https://doi.org/10.1080/25765299.2019.1607995

Anderson, G., & Shenkar, N. (2021). Potential effects of biodegradable single-use items in the sea: Polylactic acid (PLA) and solitary ascidians. *Environmental Pollution*, *268*, Article 115364. https://doi.org/10.1016/j.envpol.2020.115364

Aworinde, A. K., Adeosun, S. O., Oyawale, F. A., Emagbetere, E., Ishola, F. A., Olatunji, O., Akinlabi, S. A., Oyedepo, S. O., Ajayi, O. O., & Akinlabi, E. T. (2020a). Comprehensive data on the mechanical properties and biodegradation profile of polylactide composites developed for hard tissue repairs. *Data in Brief*, *32*, Article 106107. https://doi.org/10.1016/j.dib.2020.106107

Aworinde, A. K., Adeosun, S. O., Oyawale, F. A., Akinlabi, E. T., & Akinlabi, S. A. (2020b). Comparative effects of organic and inorganic bio-fillers on the hydrophobicity of polylactic acid. *Results in Engineering*, *5*, 1-3. https://doi.org/10.1016/j.rineng.2020.100098

Aworinde, A. K., Adeosun, S. O., & Oyawale, F. A. (2020c). Mechanical properties of poly(L-Lactide)-based composites for hard tissue repairs. *International Journal of Innovative Technology and Exploring Engineering (IJITEE)*, *9*(5), 2152-2155. https://doi.org/10.35940/ijitee.C8501.039520

Aworinde, A. K., Adeosun, S. O., Oyawale, F. A., Akinlabi, E. T., & Akinlabi, S. A. (2019). The strength characteristics of chitosan- and titanium-poly(L-lactic) acid based composites. *Journal of Physics: Conference Series*, *1378*(2), Article 022061. https://doi.org/10.1088/1742-6596/1378/2/022061

Aworinde, A. K., Adeosun, S. O., Oyawale, F. A., Akinlabi, E. T., & Emagbetere, E. (2018, October 29 - November 1). Mechanical strength and biocompatibility properties of materials for bone internal fixation: A brief overview. In *Proceedings of the International Conference on Industrial Engineering and Operations Management* (pp. 2115-2126). Pretoria, South Africa.

Aworinde, A. K., Taiwo, O. O., Adeosun, S. O., Akinlabi, E. T., Jonathan, H., Olayemi, O. A., & Joseph, O. O. (2021a). Biodegradation profiles of chitin, chitosan and titanium reinforced polylactide biocomposites as scaffolds in bone tissue engineering. *Arab Journal of Basic and Applied Sciences*, *28*(1), 351-359. https://doi.org/10.1080/25765299.2021.1971865

Aworinde, A. K., Emagbetere, E., Adeosun, S. O., & Akinlabi, E. T. (2021b). Polylactide and its composites on various scales of hardness. *Pertanika Journal of Science and Technology*, *29*(2), 1313-1322. https://doi.org/10.47836/pjst.29.2.34

Bakar, M. S. A., Cheang, P., & Khor, K. A. (2003). Mechanical properties of injection molded hydroxyapatite-polyetheretherketone biocomposites. *Composites Science and Technology*, *63*, 421-425. https://doi.org/10.1016/S0266-3538(02)00230-0

Barkhad, M. S., Abu-Jdayil, B., Mourad, A. H. I., & Iqbal, M. Z. (2020). Thermal insulation and mechanical properties of polylactic acid (PLA) at different processing conditions. *Polymers*, *12*(9), 1-16. https://doi.org/10.3390/POLYM12092091

Bouzouita, A., Notta-cuvier, D., Raquez, J., Lauro, F., & Dubois, P. (2017). Poly(lactic acid)-based materials for automotive applications. In M. L. Di Lorenzo & R. Androsch (Eds.), *Industrial Applications of Poly(lactic acid)* (pp. 177-219). Springer. https://doi.org/10.1007/12

Brischetto, S., & Torre, R. (2020). Tensile and compressive behavior in the experimental tests for PLA specimens produced via fused deposition modelling technique. *Journal of Composites Science*, *4*(3), Article 140. https://doi.org/10.3390/jcs4030140

Cooper, T. A. (2013). Developments in bioplastic materials for packaging food, beverages and other fast-moving consumer goods. In N. Farmer (Ed.), *Trends in Packaging of Food, Beverages and Other Fast-Moving Consumer Goods (FMCG)* (pp. 58-107). Woodhead Publishing Limited. https://doi.org/10.1533/9780857098979.108

Deepthi, S., Sundaram, M. N., Kadavan, J. D., & Jayakumar, R. (2016). Layered chitosan-collagen hydrogel/aligned PLLA nanofiber construct for flexor tendon regeneration. *Carbohydrate Polymers*, *153*, 492-500. https://doi.org/10.1016/j.carbpol.2016.07.124

Fang, Q., & Hanna, M. A. (1999). Rheological properties of amorphous and semicrystalline polylactic acid polymers. *Industrial Crops and Products*, *10*(1), 47-53. https://doi.org/10.1016/S0926-6690(99)00009-6

Farah, S., Anderson, D. G., & Langer, R. (2016). Physical and mechanical properties of PLA, and their functions in widespread applications - A comprehensive review. *Advanced Drug Delivery Reviews*, *107*, 367-392. https://doi.org/10.1016/j.addr.2016.06.012

Ferrer, G. G., Liedmann, A., Niepel, M. S., Liu, Z. M., & Groth, T. (2018). Tailoring bulk and surface composition of polylactides for application in engineering of skeletal tissues. *Advances in Polymer Science*, *282*, 79-108. https://doi.org/10.1007/12_2017_26

Gbenebor, O. P., Akpan, E. I., Atoba, R. A., Adeosun, S. O., Olaleye, S. A., Taiwo, O. O., Igogori, E. A., Alamu, O. B., & Aworinde, A. K. (2018). Development and performance analysis of high voltage generator for electrospinning of nano fibres. *Unilag Journal of Medicine, Science and Technology*, *6*(2), 45-58. https://doi.org/10.1520/acem20170008

Gbenebor, O. P., Atoba, R. A., Akpan, E. I., Aworinde, A. K., Adeosun, S. O., & Olaleye, S. A. (2018). Study on polylactide-coconut fibre for biomedical applications. In *Minerals, Metals and Materials Series* (pp. 263-273). Springer. https://doi.org/10.1007/978-3-319-72526-0_24

Hadasha, W., & Bezuidenhout, D. (2018). Poly(lactic acid) as biomaterial for cardiovascular devices and tissue engineering applications. *Advances in Polymer Science*, *282*, 51-77. https://doi.org/10.1007/12_2017_27

Jamshidian, M., Tehrany, E. A., Imran, M., Jacquot, M., & Desobry, S. (2010). Poly-lactic acid: Production, applications, nanocomposites, and release studies. *Comprehensive Reviews in Food Science and Food Safety*, *9*(5), 552-571. https://doi.org/10.1111/j.1541-4337.2010.00126.x

Lascano, D., Moraga, G., Ivorra-Martinez, J., Rojas-Lema, S., Torres-Giner, S., Balart, R., Boronat, T., & Quiles-Carrillo, L. (2019). Development of injection-molded polylactide pieces with high toughness by the addition of lactic acid oligomer and characterization of their shape memory behavior. *Polymers*, *11*(12), Article 2099. https://doi.org/10.3390/polym11122099

Lawrence, S. S., Willett, J. L., & Carriere, C. J. (2001). Effect of moisture on the tensile properties of poly(hydroxy ester ether). *Polymer*, *42*(13), 5643-5650. https://doi.org/10.1016/S0032-3861(00)00836-3

Li, J., Ding, J., Liu, T., Liu, J. F., Yan, L., & Chen, X. (2018). Poly(lactic acid) controlled drug delivery. *Advances in Polymer Science*, *282*, 109-138. https://doi.org/10.1007/12_2017_11

Malinconico, M., Vink, E. T. H., & Cain, A. (2018). Applications of poly(lactic acid) in commodities and specialties. *Advances in Polymer Science*, *282*, 35-50. https://doi.org/10.1007/12_2017_29

Mansour, G., Zoumaki, M., Tsongas, K., & Tzetzis, D. (2020). Starch-sandstone materials in the construction industry. *Results in Engineering*, *8*, Article 100182. https://doi.org/10.1016/j.rineng.2020.100182

Mofokeng, J. P., Luyt, A. S., Tábi, T., & Kovács, J. (2012). Comparison of injection moulded, natural fibre-reinforced composites with PP and PLA as matrices. *Journal of Thermoplastic Composite Materials*, *25*(8), 927-948. https://doi.org/10.1177/0892705711423291

Nagarajan, V., Mohanty, A. K., & Misra, M. (2016). Perspective on polylactic acid (PLA) based sustainable materials for durable applications: Focus on toughness and heat resistance. *ACS Sustainable Chemistry and Engineering*, *4*(6), 2899-2916. https://doi.org/10.1021/acssuschemeng.6b00321

Noori, H. (2019). Interlayer fracture energy of 3D-printed PLA material. *International Journal of Advanced Manufacturing Technology*, *101*(5-8), 1959-1965. https://doi.org/10.1007/s00170-018-3031-5

Oksiuta, Z., Jalbrzykowski, M., Mystkowska, J., Romanczuk, E., & Osiecki, T. (2000). Mechanical and thermal properties of polylactide (PLA) composites modified with Mg, Fe, and polyethylene (PE) additives. *Polymers*, *12*, 1-14. https://doi.org/10.3390/polym12122939

Rahimizadeh, A., Kalman, J., Henri, R., Fayazbakhsh, K., & Lessard, L. (2019). Recycled glass fiber composites fromwind turbine waste for 3D printing feedstock: Effects of fiber content and interface on mechanical performance. *Materials*, *12*(23), Article 3929. https://doi.org/10.3390/MA12233929

Rahimizadeh, A., Tahir, M., Fayazbakhsh, K., & Lessard, L. (2020). Tensile properties and interfacial shear strength of recycled fibers from wind turbine waste. *Composites Part A: Applied Science and Manufacturing*, *131*, Article 105786. https://doi.org/10.1016/j.compositesa.2020.105786

Rodrigues, N., Benning, M., Ferreira, A. M., Dixon, L., & Dalgarno, K. (2016). Manufacture and characterisation of porous PLA scaffolds. *Procedia CIRP*, *49*, 33-38. https://doi.org/10.1016/j.procir.2015.07.025

Rokbani, H., & Ajji, A. (2018). Rheological properties of poly(lactic acid) solutions added with metal oxide nanoparticles for electrospinning. *Journal of Polymers and the Environment*, *26*(6), 2555-2565. https://doi.org/10.1007/s10924-017-1155-6

Song, X., Chen, Y., Xu, Y., & Wang, C. (2014). Study on tough blends of polylactide and acrylic impact modifier. *BioResources*, *9*(2), 1939-1952. https://doi.org/10.15376/biores.9.2.1939-1952

Sun, B., Liu, H., Zhou, S., & Li, W. (2014). Evaluating the performance of polynomial regression method with different parameters during color characterization. *Mathematical Problems in Engineering*, *2014*(3), 1-8. https://doi.org/10.1155/2014/418651

Sundar, N., Stanley, S. J., Kumar, S. A., Keerthana, P., & Kumar, G. A. (2021). Development of dual purpose, industrially important PLA-PEG based coated abrasives and packaging materials. *Journal of Applied Polymer Science*, *138*(21), 1-18. https://doi.org/10.1002/app.50495

Tajitsu, Y. (2017). Poly(lactic acid) for sensing applications. In M. L. Di Lorenzo & R. Androsch (Eds.), *Industrial Applications of Poly(lactic acid)* (pp. 159-176). Springer. https://doi.org/10.1007/12

Taleb, K., Pillin, I., Grohens, Y., & Saidi-Besbes, S. (2021). Polylactic acid/Gemini surfactant modified clay bio-nanocomposites: Morphological, thermal, mechanical and barrier properties. *International Journal of Biological Macromolecules*, *177*, 505-516. https://doi.org/10.1016/j.ijbiomac.2021.02.135

Tyler, B., Gullotti, D., Mangraviti, A., Utsuki, T., & Brem, H. (2016). Polylactic acid (PLA) controlled delivery carriers for biomedical applications. *Advanced Drug Delivery Reviews*, *107*, 163-175. https://doi.org/10.1016/j.addr.2016.06.018

Wang, Z., Wang, Y., Ito, Y., Zhang, P., & Chen, X. (2016). A comparative study on the *in vivo* degradation of poly(L-lactide) based composite implants for bone fracture fixation. *Scientific Report*, *6*, 1-12. https://doi.org/10.1038/srep20770

Williams, J. G., & Gamonpilas, C. (2008). Using the simple compression test to determine Young's modulus, Poisson's ratio and the Coulomb friction coefficient. *International Journal of Solids and Structures*, *45*(16), 4448-4459. https://doi.org/10.1016/j.ijsolstr.2008.03.023

Xu, P., Ma, J., Zhang, M., Ding, Y., & Meng, L. (2018). Fracture energy analysis of concrete considering the boundary effect of single-edge notched beams. *Advances in Civil Engineering*, *2018*, Article 3067236. https://doi.org/10.1155/2018/3067236

Ye, J. J., & Zhou, J. (2013). Minimizing the condition number to construct design points for polynomial regression models. *Society for Industrial and Applied Mathematics*, *23*(1), 666-686. https://doi.org/10.1137/110850268